

The effect of hair on auditory localization cues

Bradley E. Treeby,^{a)} Jie Pan, and Roshun M. Paurobally

*Centre for Acoustics, Dynamics and Vibration, School of Mechanical Engineering,
The University of Western Australia, 35 Stirling Highway, Crawley, WA 6009, Australia*

(Received 14 May 2007; revised 15 August 2007; accepted 31 August 2007)

Previous empirical and analytical investigations into human sound localization have illustrated that the head-related transfer function (HRTF) and interaural cues are affected by the acoustic material properties of the head. This study utilizes a recent analytical treatment of the sphere scattering problem (which accounts for a hemispherically divided surface boundary) to investigate the contribution of hair to the auditory cues below 5 kHz. The hair is modeled using a locally reactive equivalent impedance parameter, and cue changes are discussed for several cases of measured hair impedance. The hair is shown to produce asymmetric perturbations to the HRTF and the interaural time and level differences. The changes in the azimuth plane are explicated via analytical examination of the surface pressure variations with source angle. Experimental HRTFs obtained using a sphere with and without a hemispherical covering of synthetic hair show a good agreement with analytical results. Additional experimental and analytical investigations illustrate that the relative contribution of the hair remains robust, regardless of the placement of the pinnas, or inclusion of a cylindrical neck. © 2007 Acoustical Society of America. [DOI: 10.1121/1.2793607]

PACS number(s): 43.66.Ba, 43.66.Pn, 43.20.Fn [KA]

Pages: 3586–3597

I. INTRODUCTION

In a natural listening environment, external sounds are predominantly coupled to the human auditory system via the pinnas and ear canals. For a given source location, the combined diffraction and reflection properties of the external human topography (i.e., the head, torso, and pinnas) create distinct timing and magnitude characteristics in the complex wave forms present at the eardrums. The rudimentary duality connecting the psychophysical interpretation of the salient features of these wave forms with the physical processes that govern their creation is well understood. The head introduces interaural time and level differences for sources offset from the median plane, the torso introduces low frequency reflections for elevated sources, and the folds and cavities of the pinnas create idiosyncratic spectral filtering effects above 3 kHz dependent on the source location (e.g., [Blauert, 1997](#); [Algazi et al., 2001a](#); [Shaw, 1997](#)). Beyond this, however, the contribution of peripheral and detailed features to the auditory percept is not well understood.

In this context, the current study serves to systematically model, describe, and explicate the effect of human terminal scalp hair on the head-related transfer function (HRTF) and related auditory localization cues. The hair is modeled as a hemispherical covering on a spherical head utilizing a recent analytical solution to the corresponding scattering problem by [Treeby et al. \(2007a\)](#). A locally reactive equivalent impedance parameter is used to encapsulate the acoustic properties of human hair as discussed by [Treeby et al. \(2007b\)](#). Cue changes are discussed for several cases of measured hair impedance. The predicted results are experimentally validated using a rigid sphere with a hemispherical covering of

synthetic hair material. The contribution of hair in relation to other peripheral features, such as the neck and pinna offset, is also investigated.

The use of spherical head models to explain features within the human HRTF is commonplace (e.g., [Kuhn, 1977](#); [Duda and Martens, 1998](#); [Brungart and Rabinowitz, 1999](#); [Algazi et al., 2002a](#)). Within certain constraints (e.g., the symmetrical and thus ambiguous directional cues), these models provide a strong theoretical foundation for understanding features within human HRTF. Such models are also utilized to reintroduce the time delays for minimum-phase HRTF reconstructions ([Kulkarni et al., 1999](#)), as the basis of structural or cascaded HRTF formations ([Brown and Duda, 1998](#); [Chan and Chen, 2000](#)), and to augment experimental HRTFs with low frequency information ([Algazi et al., 2002b](#); [Zotkin et al., 2003](#); [2006](#)).

The traditional spherical head model assumes that the scattering surfaces are completely rigid in nature. This is consistent with the general agreement that skin is sufficiently rigid throughout the audible frequency range ([Katz, 2000](#)). However, results from an earlier analytical study by [Treeby et al. \(2007d\)](#) (using a spherical head model with uniformly distributed acoustic properties) suggest that impedance values representative of human hair can introduce noticeable modifications to the interaural azimuth cues. Empirical studies using mannequins ([Riederer, 2005](#)), spheres ([Treeby et al., 2007c](#)), and the boundary element method ([Katz, 2001](#)) have also shown that the addition of hair introduces asymmetrical perturbations to the HRTF in the order of several decibels. The assumption of a uniformly distributed (and rigid) surface boundary in spherical head models (to allow for an analytic solution) precludes their use for investigation or inclusion of these features. The recent analytical development discussed by [Treeby et al. \(2007a\)](#), however, provides a scattering model for a sphere with a hemispherically split

^{a)}Electronic mail: treebs@mech.uwa.edu.au

surface boundary condition. This impedance distribution assimilates the general characteristics of a human head with hair, and thus facilitates an analytical investigation into the effect of hair on the auditory localization cues.

Considering the complexity of everyday auditory environments, there are a multitude of environmental and intrapersonal variations that may cause subtle changes to the encoded auditory cues for a particular source direction. Variations in clothing, headwear, and complex interactions with the architectural surroundings all produce changes to the available spectral features. Nevertheless, this does not necessarily mean that the ability to localize sounds is significantly perturbed. In the absence of methodical and robust psychoacoustic testing, the effect of these variations is best discussed in relation to the magnitude of their effect on the monaural and interaural cues, in combination with the resolution of the auditory system to recognize these changes. The effect of human hair to the auditory percept is discussed here in relation to these thresholds.

Published values for just-noticeable-difference (JND) changes in the interaural time difference (ITD) vary depending on the frequency content of the sound stimulus and the reference ITD used [see [Akeroyd \(2006\)](#) for a recent review]. Additional variations result from slight differences in the definition of the JND threshold (typically 75% correct), the stimulus duration, significant intersubject variability, and the stimulus encoding (whether the stimuli contains onset, offset, or an ongoing ITD). Optimum values of JND can be as low as 10 μ s, although certain subjects may exhibit JNDs well beyond this value. Removing one outlying subject, [Mossop and Culling \(1998\)](#) report broadband ITD JNDs on the order of 19 μ s for a 0 μ s reference ITD (frontal source). This increases to 72 μ s for a 600 μ s reference ITD (source near the interaural axis). Equivalent studies of the interaural level difference (ILD) JND consistently report values on the order of 1 dB (e.g., [Mills, 1958](#); [Hershkowitz and Durlach, 1969](#); [Domnitz and Colburn, 1977](#); [Hartmann and Constan, 2002](#); [Bernstein, 2004](#)). The JND is approximately independent of frequency and has only a weak dependence on the ITD reference. The corresponding minimum audible angle is 1° to 2° under optimum circumstances. This resolution intuitively decreases for source angles away from the median axis, for vertical plane localization, and for localization in the presence of noise ([Stern et al., 1983](#); [Grantham et al., 2003](#)). Detection of the direction of movement generally has a higher threshold than the detection of movement ([Chandler and Grantham, 1992](#)).

II. EXTRACTION OF LOCALIZATION CUES

For a spherical head without pinnas or ear canals, the auditory cues are simply dependent on the surface pressure at the equivalent pinna locations. This pressure is calculated here using the analytical result described by [Treeby et al. \(2007a\)](#) assuming a planar incident wave. The formulation assumes that the surface of the spherical scatterer is divided into two hemispheres, each with a uniformly distributed, locally reacting surface impedance [the validity of a locally reactive surface assumption for human hair is discussed by

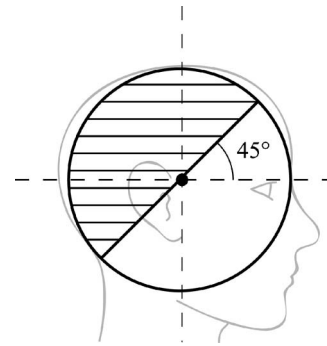


FIG. 1. Sphere scattering model with a hemispherically divided surface covering used to approximate the contribution of hair to the auditory percept. The black dot illustrates the pinna location.

[Treeby et al. \(2007b\)](#)]. If a unity source strength is assumed, at the appropriate surface locations, the complex pressure calculated by this formulation directly corresponds to the HRTF.

The simulated results presented here are based on scattering model parameters representative of human anthropometry. The sphere radius is assumed to be 8.75 cm, the hemispherical impedance boundary (hairline) elevated 45° from the median axis, and the pinnas located in the azimuth plane, offset from the frontal median axis by 90° (see Fig. 1). The symmetric alignment of the hairline and pinnas is chosen so that any asymmetries arising due to the hair covering are easier to distinguish. The effect of the pinna offset in relation to the contribution of hair is discussed in Sec. V A. The lower (facial) hemisphere is assumed to be rigid and the upper hemisphere given several representative values of complex impedance. These regions correspond to the shaded (absorbent) and unshaded (rigid) hemispheres shown in Fig. 1. The calculation of the spherical angles required by the scattering model (which assumes the hemispherical boundary to be coincident with the x - y plane) is facilitated using coordinate system transformation via Euler rotation. This allows the angles for circumferential angular sweeps outside of the axial planes to be easily calculated.

The HRTF typically exhibits idiosyncratic features for source movement throughout three-dimensional space. However, in the absence of more convenient ways to display higher dimensional data, characteristics are normally discussed in relation to source angles within the three elemental planes. For the chosen symmetric hair and pinna alignment, with an appropriate angular remapping the frontal plane is identical to the azimuth plane. Consequently, only changes within the azimuth and median planes will be considered, with the displayed data and discussion corresponding to the head's right ear. These elemental planes are shown in Fig. 2. Whilst the sphere used is pinna-less, the term "ear" is used here to denote the evaluation location in lieu of a more satisfactory description.

The HRTF pairs for left and right pinnas collectively embody the localization cues produced by the spherical head model. However, at lower frequencies it is the interaural cues rather than the monaural spectral details that are of most importance to localization. It is thus appropriate to also examine the effect of hair on these cues. The interaural cues for

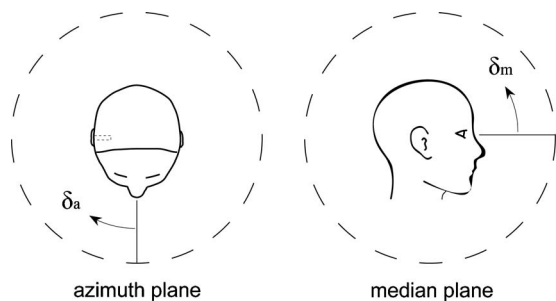


FIG. 2. Spatial reference planes and relative source rotation angles (starting from 0°). For the symmetric hair and pinna alignment used, the frontal plane is identical to the azimuth plane with the appropriate angular remapping.

a particular source location are extracted from the difference in HRTF magnitude and phase information between the two ears. The actual analytical value of ITD differs slightly depending on the method used to extract this disparity (e.g., [Treeby et al., 2007d](#)). The ITD is calculated here using the interaural phase delay. To account for the changes in ITD with frequency, the ITD trends at two characteristic frequencies are discussed (375 and 3000 Hz). These lie within the low and high frequency ITD limits described by [Kuhn \(1977\)](#). Due to the symmetry of the hair covering and pinnas about the median sagittal plane, there is no change in the interaural cues with source movement through the median plane. Changes to the interaural cues are thus only discussed in relation to the azimuth plane.

III. THE EFFECT OF IMPEDANCE ON LOCALIZATION CUES

A. Changes to the head-related transfer function

The changes to the azimuthal and median plane HRTF due to the inclusion of hair are shown in Fig. 3. For convenience, this and all subsequent results discussed in Secs. III A–III C assume a frequency independent hair impedance of $|\zeta|=2$, $\angle\zeta=45^\circ$ (where ζ is the specific acoustic impedance for normal incidence). This corresponds to a relatively dense and absorbent hair surface, and is consistent with the impedance values utilized and discussed by [Treeby et al. \(2007d; a\)](#). Whilst this selection overestimates the magnitude of some changes, it also makes the characteristic trends easier to distinguish. At low frequencies (where hair is much less absorbent), the frequency independent nature of the assumed impedance value produces particularly exaggerated results. Comparative changes and discussion using measured values of hair impedance are provided in Sec. III D. The left panels of Fig. 3 correspond to azimuthal HRTF, and the upper panels to responses for a rigid sphere. As expected, the rigid azimuthal HRTF exhibits a prominent posterior bright spot at 270° and is symmetrical about this angle. Two pronounced ridges of decreased pressure are evident adjacent to this bright spot. As the wavelength is reduced, the in-and-out of phase oscillations that arise due to interactions between symmetric wave paths occur over a shorter spatial distance. Consequently, additional lobes also become apparent at higher frequencies over approximately the same angular re-

gion. For a uniformly distributed surface boundary, moving the source angle around the sphere is equivalent to moving the ear location. The features displayed in the rigid sphere HRTF are thus identical to the stacked surface pressure plot for a rigid sphere discussed by [Treeby et al. \(2007a\)](#).

The central panels of Fig. 3 show the HRTF including hair, and the lower panels the decomposed contribution of the hair covering (calculated by subtracting the rigid response). When the hair is included, the azimuthal HRTF is noticeably perturbed. Significant changes are evident for contralateral angles adjacent to the bright spot. The primary anterior contralateral ridge of reduced pressure ($\sim 280^\circ$) is further decreased (~ 10 dB) relative to the HRTF for a rigid boundary, whilst the posterior ridge ($\sim 260^\circ$) is slightly increased. This results in a significant asymmetry about the contralateral bright spot, with the ridge of decreased pressure noticeably more apparent on the anterior side. The magnitude of the additional anterior contralateral pressure oscillations is also increased, although they oscillate about the same position. In the posterior region, these additional oscillations see a relative positive shift.

The asymmetrical contralateral HRTF changes can be explained by examining the circumferential surface pressure as the source moves around the sphere. Figure 4 shows this pressure magnitude at 2000 Hz for eight angles of source incidence. For contralateral source angles near the interaural axis, the surface pressure is asymmetrical with the primary bright spot lobe favoring the absorbent hemisphere. This is consistent with discussion given by [Treeby et al. \(2007a\)](#). The adjacent pressure nulls are also asymmetrical with the magnitude substantially less on the anterior side, particularly with reference to the equivalent rigid sphere pressure. This explains why the contralateral ridge of decreased pressure evident in the HRTF is more noticeable on the anterior side. The angular locations of the pressure nulls adjacent to the bright spot evident in Fig. 4 for a source angle of 270° are also asymmetric in rotational angle, with the anterior null appearing closer to the interaural axis. This accounts for the relative shift in the contralateral ridges seen in Fig. 3.

In addition to the changes about the contralateral bright spot, HRTF variations are also evident for ipsilateral angles. For the complex impedance phase angle shown in Figs. 3 and 4, this region remains reasonably uniform. However, when the impedance phase angle is decreased, these changes become more perceptible (further discussion on the relationship between hair properties and impedance is given in Sec. III D). For posterior ipsilateral source angles, there is a general decrease in the HRTF magnitude. This decrease is a result of the increased absorption of the frontal surface seen by the source. Again, the changes are asymmetrical about the interaural axis. For certain values of hair impedance, the disparity between anterior and posterior ipsilateral regions can be on the order of several decibels.

HRTF changes in the median plane due to hair are illustrated in the right panels of Fig. 3. For a uniform surface boundary and symmetric pinna alignment, there is no change in the HRTF with source angle. When the hemispherical hair covering is added, asymmetries are created in the scattering surface and HRTF changes are consequently established.

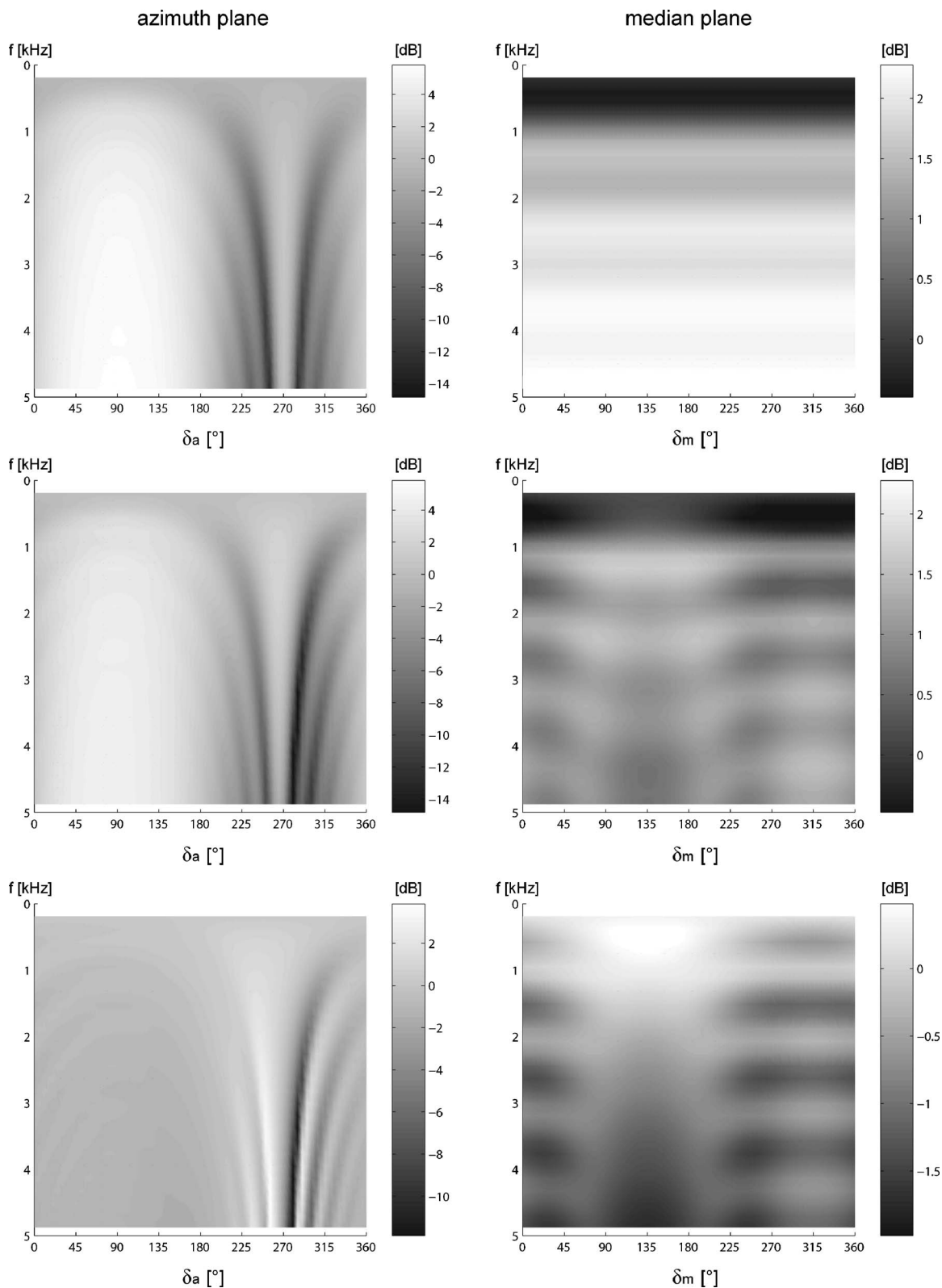


FIG. 3. Changes in the right ear head-related transfer function (HRTF) due to the addition of a hemispherical hair covering with a specific acoustic impedance of $|\zeta|=2$, $\angle\zeta=45^\circ$. The left panels display the azimuthal HRTF and the right panels the median HRTF. The upper panels correspond to a rigid sphere, the central panels include a hemispherical hair covering, and the lower panels show the decomposed HRTF change due to the hair covering.

There is a general decrease in the HRTF magnitude on the order of 1 to 2 dB. This becomes augmented as frequency increases. The changes are symmetric about 135° (or 315°), which corresponds to an axially incident source with refer-

ence to the coordinate system of the scattering model. Overall, the perturbations provided by the hair covering in the median plane are comparable in magnitude to those introduced by the sphere itself.

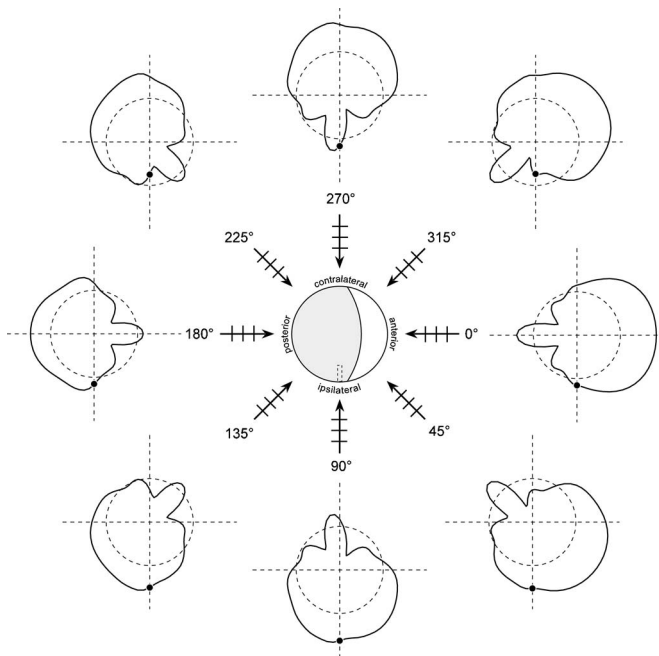


FIG. 4. Azimuthal circumferential surface pressure magnitudes at 2000 Hz for eight angles of source incidence for a spherical head with a hemispherical hair covering (where $|\zeta|=2$, $\angle\zeta=45^\circ$). The black dot on the polar plots corresponds to the pressure at the right ear and the dashed lines illustrate the polar axes and the unit circle for reference.

The general effect of hair on the azimuthal HRTF discussed here is in good agreement with experimental results presented by [Treeby *et al.* \(2007c\)](#) using a rigid spherical head and a hemispherical hair covering. The discussion is also in good agreement with experimental results presented by [Riederer \(2005\)](#), who examined the contribution of several hair coverings on the HRTF of a mannequin. The resolution and frequency range of Riederer's results make direct comparison of data below 5 kHz difficult, however, the general features are clearly evident. There is an increased disparity between the primary pressure nulls adjacent to the contralateral bright spot. For the right ear, this corresponds to a decrease for anterior contralateral angles and a slight increase for posterior, consistent with the present discussion. At higher frequencies, the asymmetric ipsilateral decrease for angles past 90° is also displayed. This posterior ipsilateral reduction becomes particularly augmented above 5 kHz. At very high frequencies (above 12 kHz), additional features are also noticeable, predominantly for posterior contralateral angles where a large decrease in the HRTF magnitude is shown. Again, the resolution of the results prohibit a more detailed explanation. Median plane changes analogous to those discussed here are not perceptible.

Only two additional studies investigating the effect of human hair are known to the authors. Preliminary results presented by [Katz \(2001\)](#) using the boundary element method illustrate that the inclusion of a nonrigid head surface introduces nontrivial variations to the HRTF. These changes are particularly noticeable for contralateral source angles on the interaural axis, consistent with the features discussed in the present study. [Wersényi and Illényi \(2005\)](#) also comment

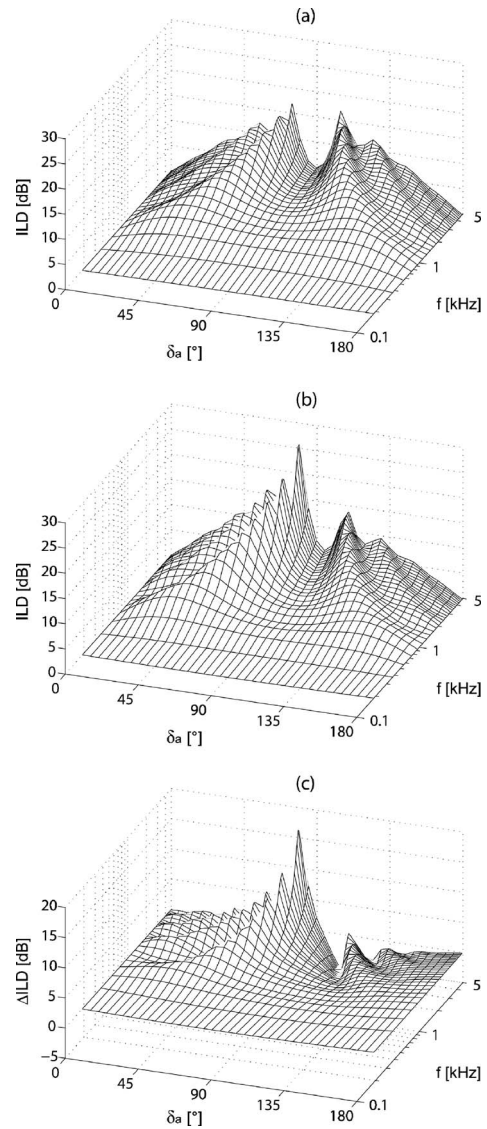


FIG. 5. Changes in the interaural level difference (ILD) due to the addition of a hemispherical hair covering (where $|\zeta|=2$, $\angle\zeta=45^\circ$), (a) ILD for a rigid sphere, (b) ILD including the hemispherical hair covering, and (c) decomposed ILD change due to the hair covering.

that the addition of a hair covering to a mannequin produces HRTF variations with frequency and source angle, including perturbation of the contralateral bright spot.

B. Changes to the interaural level difference

The changes to the ILD due to the addition of a hemispherical hair covering are reasonably intuitive given the previous discussion on the changes to the HRTF magnitude. The left ear response is a reflection of that from the right, and the ILD the difference between these. Figure 5 illustrates the corresponding ILD plots. Given the symmetric pinna alignment, for a rigid sphere [Fig. 5(a)] the ILD is symmetric about 90° . The general decrease in level difference for this angle is a result of the contralateral ear being coincident with the principal bright spot. Due to the symmetry of the scatterer about the median plane, ILDs for source angles past 180° are simply a reflection of those shown in Fig. 5. When the hair covering is added, the asymmetries present in the

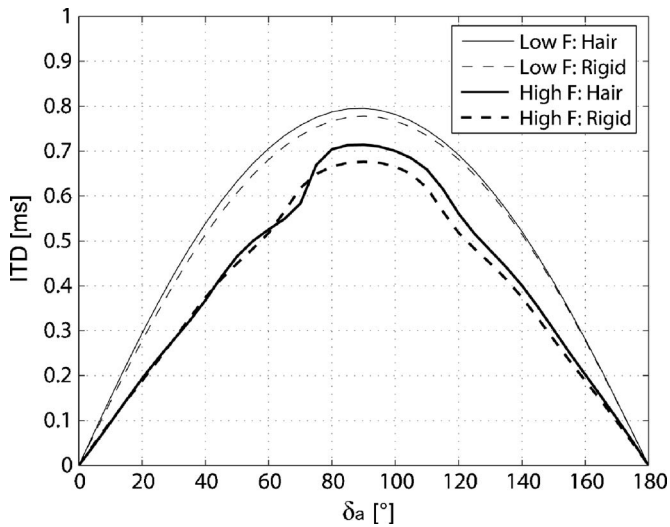


FIG. 6. Low (375 Hz) and high (3000 Hz) frequency interaural time differences (ITD) derived from a spherical head model either completely rigid ($\zeta=\infty$) or with a hemispherical hair covering ($|\zeta|=2, \angle\zeta=45^\circ$).

HRTF also cause the ILD to become asymmetrical. The corresponding ILD is shown in Fig. 5(b), with the decomposed changes due to the hair covering shown in Fig. 5(c). There is an increase in the ILD for source angles where the contralateral ear (left) coincides with a ridge of decreased pressure that has been further decreased. As the source moves past 90° , the contralateral ear coincides with a decreased pressure ridge that has been slightly increased, and the ILD is thus reduced. The asymmetry of the contralateral HRTF ridges with rotation angle also shifts the location of the 90° ILD minimum to source angles slightly posterior of the interaural axis.

C. Changes to the interaural time difference

When the surface is not rigid and the impedance is complex, the surface velocity is no longer in phase with the incoming pressure oscillations. As the ITD is dependent on the relative phase between two separate locations on the head (sphere), a shift in phase of the overall surface pressure at these locations will alter the ITD. Figure 6 shows the relative phase delays for both a rigid sphere and one including the hemispherical hair covering. The upper curves show the ITD at low frequency (375 Hz) and the lower curves at high frequency (3000 Hz). The low frequency ITD shows an increase due to the hair, but when using representative frequency dependent impedance characteristics, this difference becomes negligible (the surface is approximately rigid at low frequencies). At high frequencies, the inclusion of the hair covering generally increases the ITD. Near the interaural axis, these changes are on the order of $30\text{--}40\ \mu\text{s}$. They are asymmetrical about 90° and are greater for source angles past 75° .

For a uniformly covered sphere, a general increase in ITD is seen with a decrease in impedance magnitude, particularly for source angles near the interaural axis (Treeby *et al.*, 2007d). The difference in ITD between a completely rigid and highly absorbent sphere ($\zeta=1$) is around $100\ \mu\text{s}$. This value corresponds to an upper bound to the ITD pertur-

bation expected from a hemispherical hair covering. As discussed by Treeby *et al.* (2007d), altering the phase angle of the impedance in either direction produces a relative reduction in the ITD. This reduction is a maximum for acute impedance phase angles and source angles near the interaural axis. For realistic impedance characteristics, this can reduce the relative ITD increase by as much as 50% (when compared to a purely resistive impedance of the same magnitude).

D. Cue changes for measured values of human hair impedance

As discussed in detail by Treeby *et al.* (2007b), the measured equivalent acoustic impedance characteristics of human hair are primarily dependent on the overall sample thickness and density. Increasing either the bulk thickness or density of the sample decreases the impedance magnitude, whilst an increase in thickness additionally produces a relative increase in the impedance phase angle. For all pragmatic modifications, the equivalent impedance retains a stiffness-like reactance, with the impedance phase angle on the order of $10^\circ\text{--}50^\circ$. Figure 7 illustrates the change in HRTF due to a hemispherical hair covering utilizing three of the measured equivalent impedance properties discussed by Treeby *et al.* (2007b). These correspond to human hair within a 20 mm sample holder at $40\ \text{kg/m}^3$ [Fig. 7(a)], a 20 mm sample holder at $80\ \text{kg/m}^3$ [Fig. 7(b)], and a 40 mm sample holder at $40\ \text{kg/m}^3$ [Fig. 7(c)]. The form of the HRTF changes for all impedance values is consistent with the discussion given in Sec. III A. The corresponding ILD changes [not shown but similar in form to those in Fig. 5(c)] are a maximum for Fig. 7(c) (thicker hair sample) and are on the order of 4 dB. These results are limited by the frequency range of the measured impedance data, but the trends shown in Fig. 5 and the experimental results presented by Riederer (2005) indicate that these changes are further augmented at higher frequencies. Given an ILD JND of approximately 1 dB, it can be concluded that the changes to the ILD due to hair are in excess of the noticeable thresholds, particularly for source locations near the interaural axis.

The corresponding high frequency ITD changes are shown in Fig. 8. For all impedance values, these changes are consistent with the discussion given in Sec. III B. Again, the changes are a maximum for the thicker sample and are on the order $20\text{--}25\ \mu\text{s}$ for source angles past 75° . These values are below the broadband ITD JND values discussed by Mossop and Culling (1998) ($43\ \mu\text{s}$ for a $400\ \mu\text{s}$ reference ITD, $72\ \mu\text{s}$ for a $600\ \mu\text{s}$ reference). Whilst some studies have published ITD JND for low frequency pure tones near the interaural axis below $20\ \mu\text{s}$ (Hershkowitz and Durlach, 1969; Domnitz and Colburn, 1977), it remains unlikely that the inclusion of hair will produce a discernible shift in source location. In combination, the overall changes to the timing and magnitude properties of the HRTF due to hair will most likely introduce subtle audible features of a spectral nature. This supposition is somewhat confirmed by localization testing completed by Riederer (2005) using mannequin HRTF with various head treatments. Untrained listeners were able to perceive minor perceptual differences for large modifica-

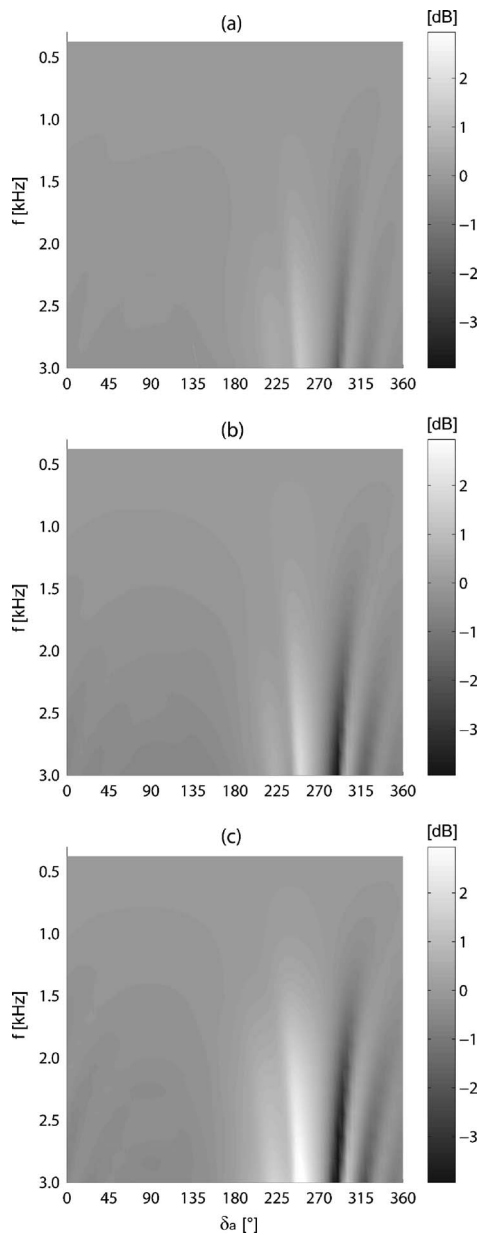


FIG. 7. Decomposed changes in the right ear HRTF due to the addition of a hemispherical covering of hair. The utilized impedance values correspond to human hair samples measured with varying sample thickness and bulk density, (a) 20 mm, 40 kg/m³, (b) 20 mm, 80 kg/m³, and (c) 40 mm, 40 kg/m³.

tions to the head covering. Overall, the inclusion of the hair did not improve localization performance (using nonindividualized HRTF), although the performance with and without hair coverings was weakly dissimilar indicating that the hair may also introduce some diminutive localization cues.

IV. EXPERIMENTAL VALIDATION OF THE IMPEDANCE SCATTERING PROBLEM

A. Experimental equipment and method

To validate the use of the hemispherical divided scattering solution to compute the auditory cue changes due to hair, a series of sphere scattering experiments were completed. These utilized a wooden sphere with an enlarged radius (12.4 cm) to obtain HRTF measurements both with and with-

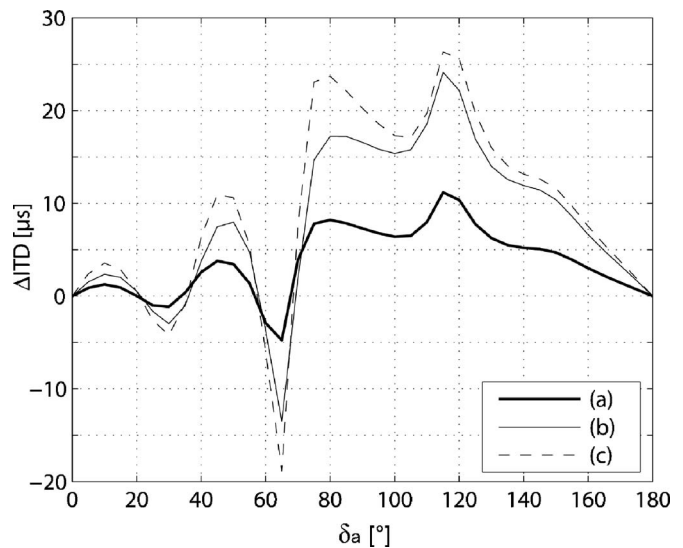


FIG. 8. Decomposed changes in the high frequency (3000 Hz) ITD due to the addition of a hemispherical hair covering to a spherical head model. The utilized impedance values correspond to human hair samples measured with varying sample thickness and bulk density, (a) 20 mm, 40 kg/m³, (b) 20 mm, 80 kg/m³, and (c) 40 mm, 40 kg/m³.

out a covering of synthetic hair material. The sphere was constructed to allow enough space (including cable relief) for two approximately diametrically opposed internal $\frac{1}{2}$ in. microphones and was supported by a thin steel rod which allowed rotation. Measurements were taken from one internal microphone (BSWA Tech MA211) which was positioned flush with the outside of the sphere surface for all experiments. All measurements were taken at 5° increments of sphere rotation starting with the internal microphone facing the frontal incident wave direction. The rotation angle was aligned using a laser level positioned at the base of the sound source (located approximately 3 m from the sphere) in conjunction with degree markings on the rotating sphere stand. The experiments were taken within an anechoic environment, and exposed areas of the stand were covered with a thick layer of highly absorbent material to minimize additional reflections.

Two series of measurements were taken starting with reference measurements of the rigid sphere. These were then repeated with the sphere hemispherically covered by a synthetic hair material. The equivalent impedance (impedance at a reference plane coincident with the inner rigid surface) and discussion of the acoustical properties of this material are given by [Treeby et al. \(2007b\)](#). The hair material came attached to a thin fabric backing and the covering was constructed from several pieces of this sewn together to make the correct shape. The covering was tailored circumspectly to maintain the overall distribution of the hair fibers, and so that it fitted neatly over the sphere surface without any significant deformation. A thin double-sided tape was used to adhere it securely. The hair line was elevated 45° from the median axis, with the internal microphone located along the hair boundary consistent with the alignment shown in Fig. 1. The hair covering was trimmed so that it did not cover the microphone as shown in Fig. 9.



FIG. 9. Experimental setup showing the wooden sphere with the synthetic hair covering. The hairline is elevated 45° and the microphone (ear) is set within the azimuth plane, offset from the frontal median axis by 90° .

For each test, impulse response measurements were obtained using maximum length sequences produced by the Brüel & Kjær DIRAC software and a Brüel & Kjær HP1001 unidirectional sound source. A sequence length of $2^{14}-1$ (the shortest available sequence length) with ten averages and a sampling frequency of 48 kHz was used. To remove the effects of the imperfectly anechoic measurement environment (the door surface was not properly treated), the impulse response peak onsets were located, and the tails then truncated to 128 samples and windowed using the second half of a cosine-tapered (Tukey) window with a 25% taper ratio. Each impulse response was then shortened to 256 samples (with

the timing information preserved) and converted to the frequency domain using a 256 point FFT. Extraction of experimental ILD and ITD information was done in the same manner as the analytical predictions.

For each of the experimental tests, comparative analytical results were derived using the equivalent impedance of the synthetic hair covering. As the experimental setup only facilitated azimuthal measurements, comparison of median plane predictions was not possible. Both experimental and analytical results were processed for frequencies from 375 to 3000 Hz. This corresponds to the available range of impedance data. Due to the enlarged radius of the test sphere, the equivalent frequency range for a head radius of 8.75 cm is 530–4250 Hz. Results shown in the following section are not frequency scaled.

B. Results for a hemispherical hair covering

Figure 10 shows the decomposed contribution of the synthetic hair covering to the HRTF and ILD. The left panels show the experimental response, and the right the corresponding analytical results. The main features of the experimental and analytical results are in good agreement and are consistent with previous discussion. The principal differences occur for posterior source angles, where the experimental HRTF changes illustrate a slightly decreased pressure magnitude and additional oscillatory behavior (evident for contralateral source angles). Consequently, the corresponding experimental and analytical results for the change in ILD also differ slightly for source angles past 90° . Predominantly, however, the analytical predictions account for the experi-

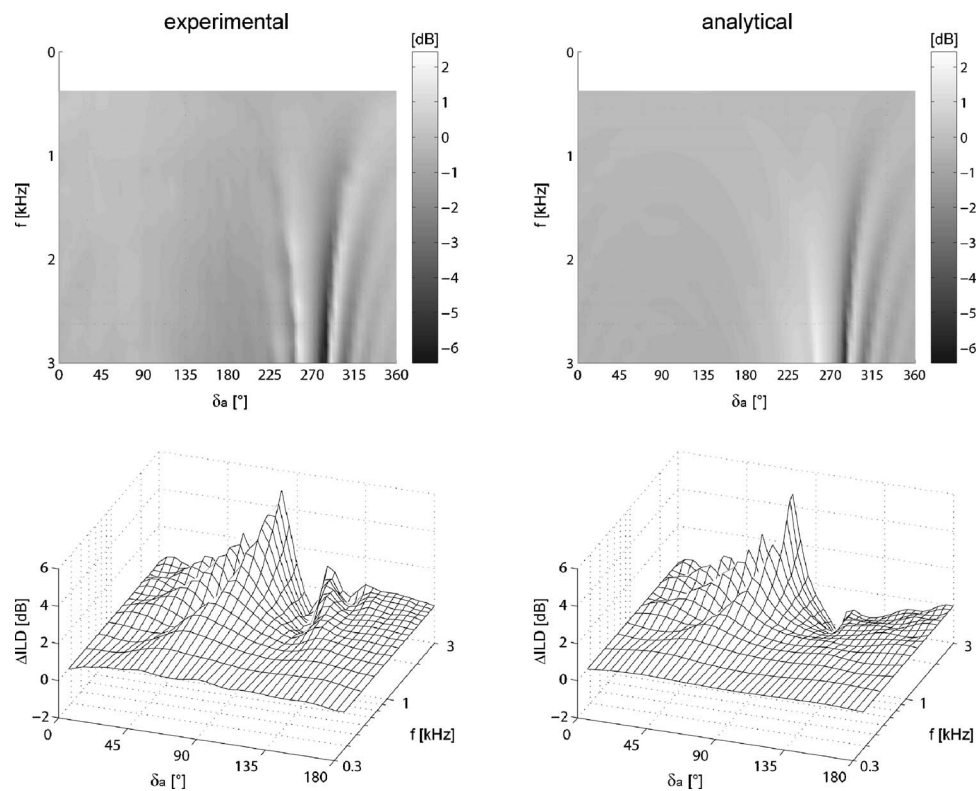


FIG. 10. Comparison of experimental (left panels) and analytical (right panels) results for the decomposed contribution of the synthetic hair material to the right ear HRTF and ILD.

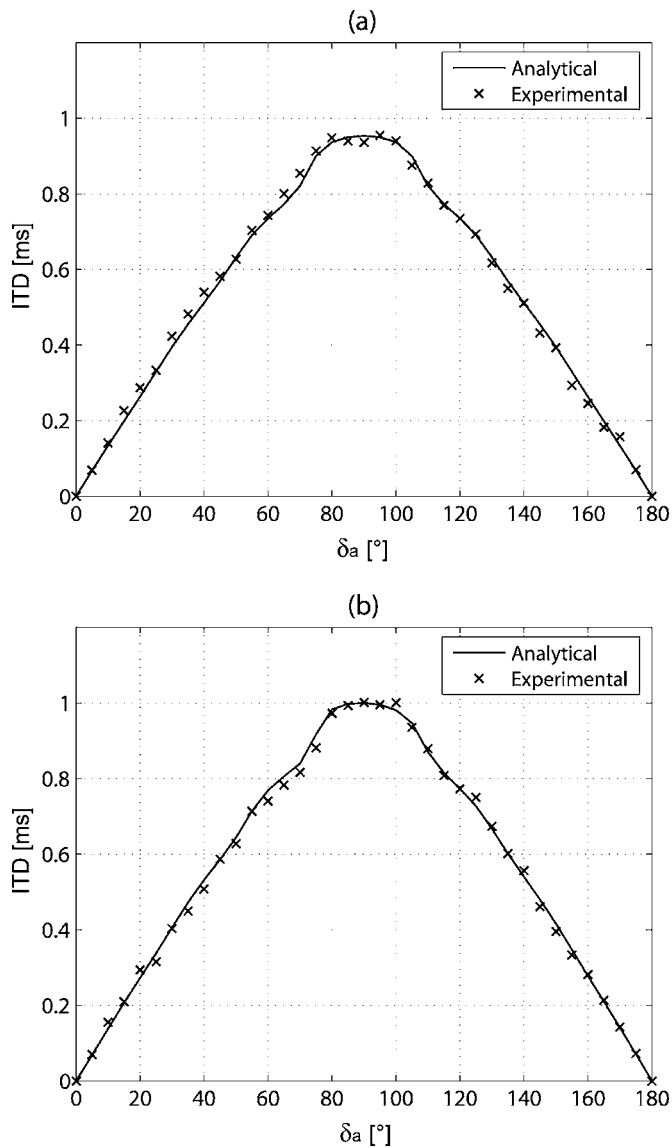


FIG. 11. Comparison of experimental and analytical values of the high frequency (3000 Hz) interaural time difference (ITD) for (a) a rigid sphere and (b) a rigid sphere with a hemispherical covering of synthetic hair.

mental changes. The variations may be attributed to slight inaccuracies in the utilized impedance characteristics of the hair covering, and experimental errors in maintaining exactly consistent rotation angles between tests with and without the hair covering. A comparison of analytical and experimental results for the high frequency ITD (3000 Hz) is shown in Fig. 11. For both the rigid sphere and the synthetic hair covering, the experimental and analytical results are in good agreement. For source angles near the interaural axis, the ITD is increased on the order of 30–50 μ s due to the addition of the hair covering. At low frequencies, the changes are negligible.

The synthetic hair sample utilized has a natural bulk density of approximately 30 kg/m³. This is at the mid to lower end of the pragmatic range expected for representative human subjects (Treeby *et al.*, 2007b). As discussed in Sec. III D, utilizing equivalent impedance values from denser or thicker hair samples yields even greater changes to the localization cues. The form of these changes, however, remains

the same, with the hair covering producing asymmetrical changes to the interaural cues between source directions in the frontal and rear hemifields. Analytical comparisons with less formal experimental measurements using an additional synthetic hair covering (which was comparatively much thicker and denser) showed that the predicted cue changes tended to underestimate the measured results. This is most likely due to the inability of the locally reactive equivalent impedance parameter to completely encapsulate the wave processes through the hair material.

V. THE CONTRIBUTION OF HAIR IN RELATION TO OTHER PERIPHERAL FEATURES

The contribution of hair to the auditory cues has thus far been discussed in relation to a single detached sphere with pinnae located on the interaural axis. Human subjects differ from this model in both head shape and pinna location. Additionally, the head is connected to other peripheral scattering bodies, for example the neck. It is important to examine whether the contribution of the hair covering remains consistent when these auxiliary features are included. The relative contributions of two additional anthropometric features are investigated in the subsequent sections. First, the effect of offsetting the pinnae to better match their physiological location is assessed. Second, the effect of connecting a semi-infinite neck to the spherical head is discussed in relation to additional experiments. The stimulus of these investigations is not to provide comprehensive discussion on the individual contributions of these ancillary features, but rather to study whether the contribution of the hair covering remains consistent and pertinent when they are included.

A. Effect of pinna offset

The location of the pinnae on an anthropometric head is commonly cited as being both downwards and backwards from the head center. For an anthropometric head shape, personalized measurements enable a relatively concise pinna position to be determined. However, when the head is modeled as a sphere this becomes considerably more complex. The spherical shape does not necessarily provide an accurate fit to the head length, width, and height measurements in isolation. Examining the relevant anthropometric data (Burkhard and Sachs, 1975; Farkas, 1981; Pheasant, 1986; Burandt *et al.*, 1991; Dreyfuss, 2002), the average ratio of auricular head height to craniofacial head height is 0.57. Assuming an 8.75 cm sphere radius, this proportionally corresponds to a 1.33 cm (8.7°) downward vertical offset of the pinnae. This offset represents the correct proportional vertical offset if the complete facial profile is taken into consideration. However, customized sphere radii are typically more dependent on the head length than the overall height of the facial profile (Algazi *et al.*, 2001b). Using the same anthropometric data, the average ratio of auricular head height to the head length is 0.68. If the sphere is aligned with the upper head surface, this ratio yields a downward vertical offset of 3.12 cm (20.9°), which is significantly more. Depending on the use for the spherical HRTF data, a value between these would most likely be appropriate. Examining

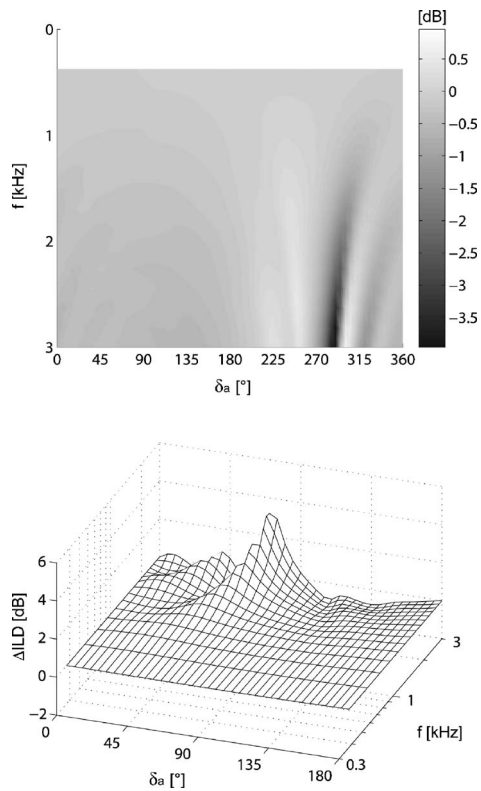


FIG. 12. The decomposed contribution of the synthetic hair material to the right ear HRTF and ILD relative to a rigid spherical head model with offset pinnae.

the horizontal offset, the average ratio of head-ear depth to head length is 0.51. Proportionally, this corresponds to a forward horizontal offset of 0.23 cm (1.5°). Assuming the same pinna position, if the sphere is aligned with the frontal head surface this becomes a backward horizontal offset of 0.46 cm (3.0°). For a spherical approximation of the head, the location of the pinnas is much closer to the interaural axis in horizontal location than in vertical. These values are consistent with [Algazi et al. \(2001a\)](#), who reported measured pinna offsets from an anthropometric mannequin for use with spherical head models to be 0.5 cm backwards and 3 cm downwards from the interaural axis (assuming a sphere radius of 8.5 cm).

To investigate the relative effect of the pinna position on the HRTF, the pinnas are assumed here to be located 10° downward and 1.5° backward of the interaural axis. This is comparable to aligning the spherical head slightly upward and forward of the geometric center of an anthropometric head. The impedance properties of the synthetic hair material are again used to characterize the contribution of hair covering. Figure 12 illustrates the decomposed effect of the hair covering in the azimuth plane relative to a rigid sphere with offset pinnas. The contribution of the hair covering remains robust regardless of the pinna offset, and the HRTF and ILD asymmetries are still clearly evident. The changes to the ITD also remain robust, with asymmetrical increases to the high frequency ITD similar in form to those shown in Figs. 6 and 8. In the median plane (not shown), the decomposed perturbations due to the hair covering are also consistent, however, the effect of the pinna offset dominates that of the hair.

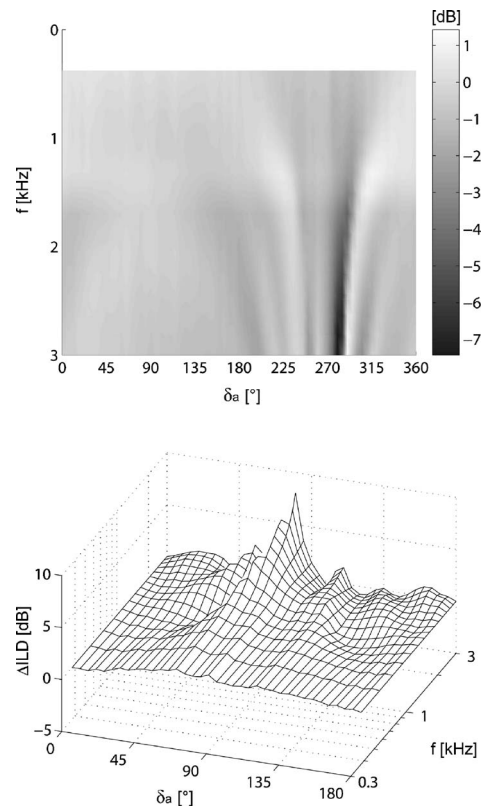


FIG. 13. Experimental changes to the right ear HRTF and ILD due to the addition of a hemispherical hair covering and a cylindrical neck to a rigid spherical head.

B. Effect of neck

If the head is examined in isolation, the major adjoining physiological features are the pinnas, face, hair, and neck. The relatively small nature of the pinnas and facial features means they contribute little to the scattering properties of the head at lower frequencies (below 3 to 4 kHz). However, it is useful to investigate the perturbation of the auditory cues by the neck, particularly in relation to the contribution of hair. [Treeby et al. \(2007c\)](#) experimentally examined the HRTF from a rigid sphere with a cylindrical neck and a hemispherical hair covering. Decomposition illustrated a reduction of the posterior bright spot due to addition of the neck on the order of 2–4 dB. This is consistent with expectations from anthropometric HRTF. The addition of the hair produced changes consistent with the discussion given here. The results from an additional but equivalent set of experiments are shown in Fig. 13. These use a 1.4 m long PVC pipe “neck” in place of the rotating sphere stand, 8 cm in radius with 1.2 cm thick walls. This corresponds to a 0.65 neck to sphere radius ratio, which is close to the anthropometric ratio of 0.675 if a 8.75 cm head radius is assumed. Whilst a 1.4 m neck does not match human physiology, it was chosen in favor of a shorter length to eliminate the effects of end scattering on the response (which also do not occur in human HRTF). Impulse response measurements were repeated for the sphere and neck arrangement, both with the hair covering and without.

The primary changes to both the HRTF and ILD shown in Fig. 13 are well explained by the individual contributions

of the two added features. There is a reduction in the contralateral bright spot due to the neck, and additional asymmetrical perturbations for both ipsilateral and contralateral angles consistent with the discussion on the effect of the hair covering. The HRTF perturbations produced by the hair are of comparable magnitude to the neck, and in the anterior contralateral region are significantly more. With regards to the ITD, the addition of the neck in isolation symmetrically reduces the overall value by up to 40 μ s. The subsequent addition of the hair produces relative ITD changes similar to those already discussed. Overall, the addition of both the neck and hair still increases the ITD, but only by a small amount (up to 20 μ s).

VI. SUMMARY AND DISCUSSION

This study utilizes a recently published analytical sphere scattering model to investigate the effect of hair on human auditory cues, a subject that has previously received little attention by the greater binaural community. The hair is shown to produce asymmetric perturbations to both the HRTF and interaural difference cues. In the azimuthal plane, the HRTF changes are characterized by two predominant features. First, the ridges of decreased pressure adjacent to the contralateral bright spot become asymmetrical, with the ridge noticeably more apparent on the anterior side. Second, for posterior ipsilateral source angles, there is a general decrease in the HRTF magnitude. This is a result of the increased absorption of the frontal surface seen by the source. Overall, the inclusion of a representative hair surface produces asymmetrical changes to the ILD and ITD on the order of 4 dB and 25 μ s, respectively (only frequencies up to 3 kHz are investigated due to the range of the available impedance data). These modifications remain robust regardless of the decomposition baseline (i.e., the inclusion of additional anthropometric features). In the azimuth plane, the addition of a cylindrical neck and the introduction of a pinna offset do not significantly influence the contribution from the hair. In the median plane, the HRTF changes introduced by the hair are similar in magnitude to those introduced by the sphere itself. However, the introduction of a pinna offset appears to modify the HRTF in this plane to a much greater extent.

The analytical results are experimentally validated using a series of azimuthal HRTF measurements from a sphere with and without a hemispherical hair covering. These results show a good agreement with analytical results for the same hair material. This mutually validates the use of the analytical formulation presented by [Treeby *et al.* \(2007a\)](#), and the equivalent impedance values given by [Treeby *et al.* \(2007b\)](#) for modeling the acoustic contribution of human hair. The additional trends in equivalent impedance for representative human hair samples discussed by [Treeby *et al.* \(2007b\)](#) subsequently allows simulation of the contribution of hair for a wide range of individuals. It should be noted that it is not difficult to think of head and hair characteristics that are not well approximated by a sphere with a hemispherically divided boundary condition (e.g., people who are partially bald, or have thick beards, etc). However, for physi-

cal understanding it is favorable to make astute simplifying assumptions that enable analytical investigation rather than attempt an exhaustive empirical study. As a sphere is only an approximation of the human head, a distribution of impedance that assimilates the general characteristics of the location of the hair is sufficient to investigate its contribution. In any case, for a large majority of people the boundary condition utilized here provides an adequate approximation. This boundary distribution may also be useful to simulate the contribution of other head coverings such as beanies (toques). Although such an addition may perturb the natural protrusion of the pinna, this is of little significance at lower frequencies.

The small magnitude of the cues produced by human hair (only the ILD changes are above JND thresholds) makes it unlikely that this topographical feature is significant in shaping the auditory percept. Given the relative plasticity of the auditory system to adapt to linear cue transformations with short term training (e.g., [Shinn-Cunningham *et al.*, 2005](#)) and complex transformations with long term training (e.g., [Hofman *et al.*, 1998](#)), the argument for including the effects of hair in auditory cue models is not strong [see [Wright and Zhang \(2006\)](#) for a recent review of auditory cue adaptation studies]. In contrast, however, for untrained listeners, even small perturbations to individualized HRTF can decrease localization accuracy within a virtual environment (e.g., [Wenzel *et al.*, 1993](#)). The contribution from hair, in combination with other peripheral and detailed features, may thus be important for accurately maintaining the spatial cues that a listener “normally” experiences. In relation to the use of spherical head models (particularly in isolation), the directional ambiguities created by the assumption of a rigid boundary limits their practical use. In this regard, the asymmetries introduced by the hair covering may assist in the discrimination between sources positioned in the front and rear hemifields. This may be particularly useful in the absence of other high frequency cues, or access to cue changes with head movement. In any case, the current study serves to clearly identify, quantify, and explicate the HRTF features that occur due to human hair.

ACKNOWLEDGMENTS

The authors would like to thank Frances Dooney for the construction of the synthetic hair covering. B.E.T. would also like to acknowledge the financial support of the Robert and Maude Gladden, and F. S. Shaw Memorial Postgraduate Scholarships.

- Akeroyd, M. A. (2006). “The psychoacoustics of binaural hearing,” *Int. J. Audiol.* **45**, S25–S33.
- Algazi, V. R., Avendano, C., and Duda, R. O. (2001a). “Elevation localization and head-related transfer function analysis at low frequency,” *J. Acoust. Soc. Am.* **109**, 1110–1122.
- Algazi, V. R., Avendano, C., and Duda, R. O. (2001b). “Estimation of a spherical-head model from anthropometry,” *J. Audio Eng. Soc.* **49**, 472–479.
- Algazi, V. R., Duda, R. O., Duraiswami, R., Gumerov, N. A., and Tang, Z. (2002a). “Approximating the head-related transfer function using simple geometric models of the head and torso,” *J. Acoust. Soc. Am.* **112**, 2053–2064.
- Algazi, V. R., Duda, R. O., and Thompson, D. M. (2002b). “The use of

- head-and-torso models for improved spatial sound synthesis," Proceedings of the 113th AES Convention, Audio Engineering Society, Los Angeles, CA, preprint 5712.
- Bernstein, L. R. (2004). "Sensitivity to interaural intensive disparities: Listeners' use of potential cues," *J. Acoust. Soc. Am.* **115**, 3156–3160.
- Blauert, J. (1997). *Spatial Hearing: The Psychophysics of Human Sound Localization* (MIT, Cambridge).
- Brown, C. P., and Duda, R. O. (1998). "A structural model for binaural sound synthesis," *IEEE Trans. Speech Audio Process.* **6**, 476–488.
- Brungart, D. S., and Rabinowitz, W. M. (1999). "Auditory localization of nearby sources. Head-related transfer functions," *J. Acoust. Soc. Am.* **106**, 1465–1479.
- Burandt, U., Posselt, C., Ambrozus, S., Hosenfeld, M., and Knauff, V. (1991). "Anthropometric contribution to standardising manikins for artificial-head microphones and to measuring headphones and ear protectors," *Appl. Ergon.* **22**, 373–378.
- Burkhard, M. D., and Sachs, R. M. (1975). "Anthropometric manikin for acoustic research," *J. Acoust. Soc. Am.* **58**, 214–222.
- Chan, C.-T., and Chen, O. T.-C. (2000). "A 3D sound using the adaptive head model and measured pinna data," *IEEE International Conference on Multimedia and Expo*, New York, pp. 807–810.
- Chandler, D. W., and Grantham, D. W. (1992). "Minimum audible movement angle in the horizontal plane as a function of stimulus frequency and bandwidth, source azimuth, and velocity," *J. Acoust. Soc. Am.* **91**, 1624–1636.
- Domnitz, R. H., and Colburn, H. S. (1977). "Lateral position and interaural discrimination," *J. Acoust. Soc. Am.* **61**, 1586–1598.
- Dreyfuss, H. (2002). *The Measure of Man and Woman: Human Factors in Design* (Wiley, New York).
- Duda, R. O., and Martens, W. L. (1998). "Range dependence of the response of a spherical head model," *J. Acoust. Soc. Am.* **104**, 3048–3058.
- Farkas, L. G. (1981). *Anthropometry of the Head and Face in Medicine* (Elsevier, New York).
- Grantham, D. W., Hornsby, B. W. Y., and Erpenbeck, E. A. (2003). "Auditory spatial resolution in horizontal, vertical, and diagonal planes," *J. Acoust. Soc. Am.* **114**, 1009–1022.
- Hartmann, W. M., and Constan, Z. A. (2002). "Interaural level differences and the level-meter model," *J. Acoust. Soc. Am.* **112**, 1037–1045.
- Hershkowitz, R. M., and Durlach, N. I. (1969). "Interaural time and amplitude jnds for a 500-Hz tone," *J. Acoust. Soc. Am.* **46**, 1464–1467.
- Hofman, P. M., Van Riswick, J. G. A., and Van Opstal, A. J. (1998). "Re-learning sound localization with new ears," *Nat. Neurosci.* **1**, 417–421.
- Katz, B. F. G. (2000). "Acoustic absorption measurement of human hair and skin within the audible frequency range," *J. Acoust. Soc. Am.* **108**, 2238–2242.
- Katz, B. F. G. (2001). "Boundary element method calculation of individual head-related transfer function. II. Impedance effects and comparison to real measurements," *J. Acoust. Soc. Am.* **110**, 2449–2455.
- Kuhn, G. F. (1977). "Model for the interaural time differences in the azimuthal plane," *J. Acoust. Soc. Am.* **62**, 157–167.
- Kulkarni, A., Isabelle, S. K., and Colburn, H. S. (1999). "Sensitivity of human subjects to head-related transfer-function phase spectra," *J. Acoust. Soc. Am.* **105**, 2821–2840.
- Mills, A. W. (1958). "On the minimum audible angle," *J. Acoust. Soc. Am.* **30**, 237–246.
- Mossop, J. E., and Culling, J. F. (1998). "Lateralization of large interaural delays," *J. Acoust. Soc. Am.* **104**, 1574–1579.
- Pheasant, S. (1986). *Bodyspace: Anthropometry, Ergonomics and Design* (Taylor and Francis, London).
- Riederer, K. A. J. (2005). "HRTF analysis: Objective and subjective evaluation of measured head-related transfer functions," Ph.D. dissertation, Helsinki University of Technology, Helsinki.
- Shaw, E. A. G. (1997). "Acoustical features of the external ear," in *Binaural and Spatial Hearing in Real and Virtual Environments*, edited by R. H. Gilkey and T. R. Anderson (Erlbaum, Mahwah), pp. 25–47.
- Shinn-Cunningham, B. G., Streeter, T., and Gyss, J.-F. (2005). "Perceptual plasticity in spatial auditory displays," *ACM T. Appl. Percept.* **2**, 418–425.
- Stern, R. M. J., Slocum, J. E., and Phillips, M. S. (1983). "Interaural time and amplitude discrimination in noise," *J. Acoust. Soc. Am.* **73**, 1714–1722.
- Treedy, B. E., Pan, J., and Paurobally, R. M. (2007a). "Acoustic scattering by a sphere with a hemispherically split boundary condition," *J. Acoust. Soc. Am.* **122**, 46–57.
- Treedy, B. E., Pan, J., and Paurobally, R. M. (2007b). "An experimental study of the acoustic impedance characteristics of human hair," *J. Acoust. Soc. Am.* **122**, 2107–2117.
- Treedy, B. E., Paurobally, R. M., and Pan, J. (2007c). "Decomposition of the HRTF from a sphere with neck and hair," Proceedings of the 13th International Conference on Auditory Display, Montreal, Canada, pp. 79–84.
- Treedy, B. E., Paurobally, R. M., and Pan, J. (2007d). "The effect of impedance on interaural azimuth cues derived from a spherical head model," *J. Acoust. Soc. Am.* **121**, 2217–2226.
- Wenzel, E. M., Arruda, M., Kistler, D. J., and Wightman, F. L. (1993). "Localization using nonindividualized head-related transfer functions," *J. Acoust. Soc. Am.* **94**, 111–123.
- Wersényi, G., and Illényi, A. (2005). "Differences in dummy-head HRTFs caused by the acoustical environment near the head," *Electronic Journal, Technical Acoustics* **1**, 1–15.
- Wright, B. A., and Zhang, Y. (2006). "A review of learning with normal and altered sound-localization cues in human adults," *Int. J. Audiol.* **45**, S92–S98.
- Zotkin, D. N., Duraiswami, R., Grassi, E., and Gumerov, N. A. (2006). "Fast head-related transfer function measurement via reciprocity," *J. Acoust. Soc. Am.* **120**, 2202–2215.
- Zotkin, D. N., Hwang, J., Duraiswami, R., and Davis, L. S. (2003). "HRTF personalization using anthropometric measurements," *IEEE Workshop on Applications of Signal Processing to Audio and Acoustics*, IEEE, New Paltz, NY, pp. 157–160.